Low threshold and high Brillouin gain coefficients of piezoelectric semiconductor magneto-plasmas

ARUN KUMAR[1], SUNITA DAHIYA[1], NAVNEET SINGH[2], MANJEET SINGH[3,*]
[1]*Department of Physics, Baba Mastnath University, Asthal Bohar, Rohtak-124021, India*
[2]*Department of Physics, Rajiv Gandhi Government College for Women, Bhiwani-127021, India*
[3]*Department of Physics, Government College, Matanhail, Jhajjar – 124106, India*

Assuming that the origin of stimulated Brillouin scattering (SBS) lies in effective Brillouin susceptibility arising due to (i) current density dependent nonlinear induced polarization, and (ii) pump wave – acoustical phonon mode dependent electrostrictive polarization; expressions are obtained for the steady-state and transient Brillouin gain coefficients of weakly-piezoelectric semiconductors magneto-plasmas under different geometrical configurations of applied magnetic field. The threshold value of pump intensity and optimum value of pulse duration for the onset of transient SBS are estimated. For numerical calculations, n-InSb crystal at 77K temperature, acting as a Brillouin medium, is assumed to be irradiated by a pulsed CO_2 laser. The influence of piezoelectric property of the Brillouin medium on threshold and Brillouin gain coefficients is analyzed. The dependence of Brillouin gain coefficients on doping concentration, applied magnetic field and its inclination, scattering angle and pump pulse duration are explored in detail with aim to determine suitable values of these controllable parameters to enhance Brillouin gain coefficients at lower pump powers, and to search the feasibility of Brillouin nonlinearities based efficient semiconductor optoelectronic devices.

(Received June 23, 2021; accepted April 8, 2022)

*Keywords :*Laser-plasma interaction, Brillouin gain, Threshold intensity, Semiconductor-plasmas

1. Introduction

Nonlinear optics is a wide area of current research owing to its important applications in fabrication of modern optoelectronic devices such as laser amplifiers and oscillators, ultra-short pulsed lasers,optical signal processing, optical sensors, optical computers, ultrafast switches and many others [1-3]. Nonlinear optical effects (NLOEs) are generally studied under two broad regimes, viz. steady-state (SS) and transient (TR) regimes. SS-NLOEs occur as a consequence of CW/pulsed laser – matter interaction such that the laser pulse duration is much longer than the recombination time of excited state carriers. Conversely, TR-NLOEs occur as a consequence of pulsed laser – matter interaction such that the laser pulse duration is much shorter than the recombination time of excited state carriers. TR-NLOEs have been observed in various nonlinear optical media after the development of femto-second lasers [4].

Among the rich variety of SS- and TR-NLOEs, stimulated Brillouin scattering(SBS) of a laser radiation has been an active area of theoretical and experimental research, since its first observation in 1964 [5]. SBS occurs as a consequence of nonlinear interaction of an intense pump wave with internally generated acoustical mode (via electrostriction or radiation pressure) of the medium. It manifests itself via generation of a forward/backward scattered Stokes wave shifted from the pump wave frequency by an amount determined by the acoustical phonon mode frequency. SBS is well known for its usage in beam shaping, pulse compression, and optical phase conjugation (OPC) [6, 7]. Brillouin-enhanced four-wave mixing (BEFWM) process yields OPC signal with extremely high reflectivity [8, 9]. SBS based optical phase conjugate mirrors (SBS-OPCMs) have been employed to cancel the aberration of coherent optical radiation generated in laser systems; thereby enhancing their overall performance. It permits usage of laser systems in various fields (such as laser induced fusion, space communication, LIDAR etc.) requiring aberration free coherent optical radiation [10]. Fiber Brillouin sensors have been developed for high-resolution/accuracy temperature sensing applications in engineering [11, 12].

SBS has been demonstrated in a variety of nonlinear optical media and hence extensive literature has accumulated on various aspects of this phenomenon. The new development of techniques for the fabrication of nonlinear materials has significantly contributed to this evolution. Among rich variety of existing nonlinear optical materials, piezoelectric semiconductor magneto-plasmas possess large optical nonlinearities and satisfy at the same time all the technological requirements for applications (such as quick response, broad transparency regime, high optical damage threshold etc.) and hence prove to be advantageous hosts for further exploration of NLOEs, including SBS [13].

Among various nonlinear optical parameters, the SS and TR Brillouin gain coefficients (BGCs) may be regarded as most important parameters characterizing SBS in a Brillouin medium. The dependence of these parameters on various affecting factors has opened up new avenues for better understanding of SBS process in Brillouin media and

performance of Brillouin nonlinearities based optoelectronic devices. SS- and TR-BGCs have been used to explore: (i) ultra-short amplification [14], pulse compression [15], and phase conjugation [9] in a Brillouin cell; (ii) frequency comb [16], beam cleanup [17], coherent beam combination [18], fast and slow light [19] in optical fibers; (iii) performance of fiber sensors [12], narrow line-width Brillouin lasers [20], and multi-wavelength fiber lasers [21]; and (iv) performance of SBS spectrometer [22] for material analysis.

We expect that the dependence of SS- and TR-BGCs on materials (piezoelectric and electrostrictive) property, applied magnetic field and doping concentration in a Brillouin cell consisting of a semiconductor will open up new ways of thinking about laser-semiconductor interactions and possibility of fabrication of efficient Brillouin amplifiers.

Up to now, SBS has been studied in semiconductor magneto-plasmas by classical, semi-classical and quantum mechanical approach [23-25]. In these studies:

(i) SBS has been studied in the SS regime, however the study of SBS under TR regime provides a better understanding of the laser-plasma interaction and idea of compression of laser pulses.

(ii) SBS has been studied by including the piezoelectric and electrostrictive coefficients phenomenologically; the role of these coefficients on Brillouin nonlinearity has not been explored. In piezoelectric semiconductor magneto-plasmas, the collective oscillation of the lattice can easily be coupled strongly with plasma wave through piezoelectricity [26]. Moreover, piezoelectricity of the medium provides the important spectral characteristics of propagation in semiconductor plasma [27]. Hence the role of SS- and TR-BGCs in analytical investigations of SBS seems to be important from the fundamental point of view.

(iii) the backward scattered Stokes mode has been considered. However, in SBS the scattered Stokes mode propagates not only in backward direction but it scatters in all possible directions. In recent years, forward SBS is becoming an emerging hot topic for the fabrication of waveguides for applications in photonic devices and hence the calculation of backward as well as forward SBS gain coefficients in analytical investigations of SBS seems to be important from the technological applications point of view [28].

(iv) the semiconductor-plasma has been magnetized by applying an external magnetic field either parallel to the pump wave propagation (Faraday geometry) or perpendicular to the pump wave propagation (Voigt geometry). However, the semiconductor-plasma can be magnetized by applying an external magnetic field in any direction (from Faraday to Voigt geometry) to the pump wave propagation.

The above discussion warrants that the phenomenon of SBS in piezoelectric semiconductor magneto-plasmas should be treated under SS as well as TR regimes. TR-BGC of a Brillouin medium, in general, is related to SS-BGC [29]. Using this approach and treating the piezoelectric semiconductor magneto-plasma as a Brillouin medium, we develop a theoretical model to study the SS- and TR-BGCs with aim to determine the role of piezoelectric and electrostrictive coefficients, external magnetic field (under various geometrical configurations) on Brillouin nonlinearity, and the backward as well as forward BGCs. Effective Brillouin susceptibility and consequent SS- and TR-BGCs are obtained following the coupled-mode approach. Numerical calculations are performed for an n-type InSb crystal duly irradiated by a pulsed 10.6 μm CO_2 laser. Efforts are directed towards to enhance SS- and TR-BGCs at lower threshold intensities by adjusting the material parameters and geometry of the applied magnetic field, and to search the feasibility of Brillouin nonlinearities based efficient semiconductor optoelectronic devices. The relevant experiment has not been performed.

2. Theoretical formulations

In this section, expressions are obtained for effective Brillouin susceptibility arising due to: (i) current density dependent nonlinear induced polarization, and (ii) pump wave – acoustical phonon mode dependent electrostrictive polarization and hence SS- and TR-BGCs, threshold pump intensity for exciting TR-SBS and the optimum value of pulse duration for the onset of TR-SBS.

2.1. Induced current density

We consider the well-known classical hydrodynamic model (valid only in the limit $k_a l \ll 1; k_a$ is the acoustical phonon mode number, and l the mean free path of charge carriers) of homogeneous semiconductor magneto-plasma under thermal equilibrium [30].

In highly doped semiconductor-plasmas, since the de-Broglie wavelength of plasma particles is much larger than the inter-fermion distances and the influence of Pauli exclusion principle, various quantum effects occur[31]. Using quantum hydrodynamic model, the variations in nonlinear characteristics of quantum semiconductor-plasmas from that of classical ones have been reported [32]. This model is helpful in analytical investigations of the short-scale collective phenomena in highly doped semiconductor-plasmas [33]. By the inclusion of statistical degeneracy pressure and quantum diffraction terms, quantum hydrodynamic model becomes a generalization of the usual fluid model. Using quantum hydrodynamic model, the study of quantum effects on SS- and TR-BGCsof semiconductor magneto-plasmas is available in literature [25, 34, 35].

SBS occurs as a consequence of nonlinear interaction among three coherent fields:

(i) an intense pump field

$$E_0(x,t) = E_0 \exp[i(k_0 x - \omega_0 t)],$$

(ii) an induced acoustical phonon (idler) mode

$$u(x,t) = u_0 \exp[i(k_a x - \omega_a t)], \text{ and}$$

(iii) a scattered Stokes component of pump (signal) field

$$E_s(x,t) = E_s \exp[i(k_s x - \omega_s t)].$$

These fields are connected via momentum and energy phase matching relations:

$$\hbar\vec{k}_0 = \hbar\vec{k}_a + \hbar\vec{k}_s \text{ and } \hbar\omega_0 = \hbar\omega_a + \hbar\omega_s,$$

respectively. The magnitudes of three wave vectors are connected via relation:

$$k_a = (k_0^2 + k_s^2 - 2k_0k_s\cos\phi)^{1/2},$$

where ϕ is the scattering angle between $\vec{k}_s$ and $\vec{k}_0$. In order to magnetize the semiconductor-plasma, we assume it to be immersed in an external magnetic field $\vec{B}_0$ in a direction making an arbitrary angle θ with the x-axis (i.e. pump wave propagation direction) in the x-z plane. The geometry of SBS in an external magnetic field is shown in Fig. 1.

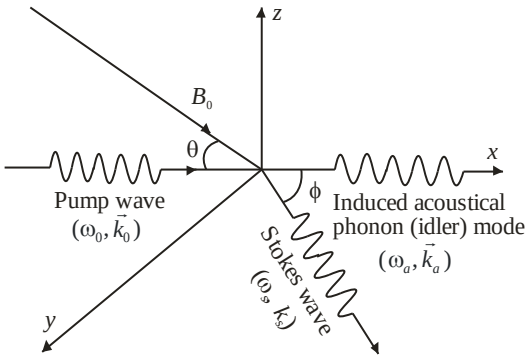

Fig. 1. Geometry of SBS in an external magnetic field

In a Brillouin active medium, let *x* be the lattice position and *u*(*x*, *t*) be the departure of lattice position from its original position so that one-dimensional strain in the direction of +*x* axis (i.e. along the pump wave propagation direction) is given by $\partial u(x,t)/\partial x$. Using Ref. [27], one may express the equation of motion of *u*(*x*, *t*) as:

$$\frac{\partial^2 u(x,t)}{\partial t^2} - \frac{C}{\rho}\frac{\partial^2 u(x,t)}{\partial x^2} + 2\Gamma_a\frac{\partial u(x,t)}{\partial t} = \frac{F_e(\beta,\gamma)}{\rho} \quad (1a)$$

where *C* is the linear elastic modulus of the crystal such that the acoustical phonon velocity is given by $v_a = (C/\rho)^{1/2}$. ρ represents the crystal mass density. In order to take account of acoustical damping, the term $2\Gamma_a\frac{\partial u(x,t)}{\partial t}$ is introduced phenomenologically. $F_e(\beta,\gamma)$ stands for the net force per unit volume accomplished by the medium in the presence pump electromagnetic field, it can be expressed as [27]:

$$F_e(\beta,\gamma) = F_\beta^{(1)} + F_\gamma^{(2)},$$

where

$F_\beta^{(1)} = -\beta\frac{\partial E_1}{\partial x}$ represents the first-order force arising due to piezoelectric property, and

$F_\gamma^{(2)} = \frac{\gamma}{2}\frac{\partial}{\partial x}(E_0E_1^*)$ stands for second-order force arising due to electrostrictive property of the Brillouin medium.

Here β and γ are piezoelectric and electrostriction coefficients of the Brillouin medium, respectively. E_1 is the space charge electric field. The asterisk (*) stands for the conjugate of a complex entity. It should be worth pointing out that in the presence of oscillating pump field the ions inside the lattice shift into non-symmetrical position, generally bringing about a contraction in the pump field direction and an expansion in a direction perpendicular to it. The electrostrictive property has its origin in the electrostrictive force thus produced in the crystal. The coupling of oscillating pump electromagnetic field and elastic properties of the lattice gives rise to piezoelectric force in the medium.

Substituting the value of $F_e(\beta,\gamma)$ in Eq. (1a)), the equation of motion of *u*(*x*, *t*) becomes

$$\frac{\partial^2 u(x,t)}{\partial t^2} - \frac{C}{\rho}\frac{\partial^2 u(x,t)}{\partial x^2} + 2\Gamma_a\frac{\partial u(x,t)}{\partial t} = -\frac{\beta}{\rho}\frac{\partial E_1}{\partial x} + \frac{\gamma}{2\rho}\frac{\partial}{\partial x}(E_0E_1^*) \quad (1b)$$

The other basic equations in the present formulation are:

$$\frac{\partial\vec{v}_0}{\partial t} + \nu\vec{v}_0 + \left(\vec{v}_0.\frac{\partial}{\partial x}\right)\vec{v}_0 = -\frac{e}{m}[\vec{E}_0 + (\vec{v}_0\times\vec{B}_0)] = -\frac{e}{m}(\vec{E}_e) \quad (2)$$

$$\frac{\partial\vec{v}_1}{\partial t} + \nu\vec{v}_1 + \left(\vec{v}_0.\frac{\partial}{\partial x}\right)\vec{v}_1 + \left(\vec{v}_1.\frac{\partial}{\partial x}\right)\vec{v}_0 = -\frac{e}{m}[\vec{E}_1 + (\vec{v}_0\times\vec{B}_0)] \quad (3)$$

$$\frac{\partial n_1}{\partial t} + n_0\frac{\partial v_1}{\partial x} + n_1\frac{\partial v_0}{\partial x} + v_0\frac{\partial n_1}{\partial x} = 0 \quad (4)$$

$$\vec{P}_{es} = -\gamma\frac{\partial u^*}{\partial x}(\vec{E}_0) \quad (5)$$

$$\frac{\partial E_1}{\partial x} + \frac{\beta}{\varepsilon}\frac{\partial^2 u}{\partial x^2} + \frac{\gamma}{\varepsilon}\frac{\partial^2 u^*}{\partial x^2}(E_0) = -\frac{n_1 e}{\varepsilon} \quad (6)$$

Eqs. (2) – (6) and the notations used are well explained in Ref. [24]. Here, $\vec{v}_0$ (n_0) and $\vec{v}_1$ (n_1) represent the equilibrium and perturbed oscillatory fluid velocities

(carrier concentrations), respectively. ν is the collision frequency of electrons. m is the electron's effective mass. e is electronic charge. $\vec{P}_{es}$ stands for nonlinear polarization originating from nonlinear interaction of pump field with acoustical vibrations of the Brillouin medium.

The forces $F_{\beta}^{(1)}$ and $F_{\gamma}^{(2)}$ create carrier (here electrons) density perturbations in the semiconductor magneto-plasma which can be obtained by using the method adopted in Ref. [24]. Differentiating Eq. (4), substituting the first-order derivatives of v_0 and v_1 from Eqs. (2) and (3), respectively;E_1 from Eq. (6) and after mathematical simplification the coupled equation of carrier density perturbations is obtained as:

$$\frac{\partial^2 n_1}{\partial t^2}+\nu\frac{\partial n_1}{\partial t}+\bar{\omega}_p^2 n_1+\frac{n_0 e k_s^2 u^*}{m\varepsilon_1}(\beta\gamma\delta_1\delta_2 A+\gamma^2 E_0^2)E_0E_s^*=in_1k_s\bar{E} \tag{7}$$

where $\bar{E}=\frac{e}{m}(\vec{E}_e)$, $A=\frac{\omega_p^2}{(e/m)k_a}$,

$\delta_1=1-\frac{\omega_c^2}{(\omega_0^2-\omega_c^2)}$, $\delta_2=1-\frac{\omega_c^2}{(\omega_s^2-\omega_c^2)}$,

$\bar{\omega}_{pc}=\nu\left(\frac{\omega_p\omega_c}{\omega_p^2+\omega_c^2}\right)$ (coupled plasmon-cyclotron frequency

$\omega_p=\left(\frac{n_0e^2}{m\varepsilon}\right)^{1/2}$ (electron-plasma frequency), and

$\omega_c=\frac{eB_0}{m}$ (electron-cyclotron frequency).

The perturbed electron concentration$n_1$may be expressed as:

$$n_1=n_{1s}(\omega_a)+n_{1f}(\omega_s),$$

wheren_{1s} (known as low frequency component) oscillates at acoustical phonon mode frequency ω_a while n_{1f} (known as high frequency component) is associated with electromagnetic waves at frequencies $\omega_0\pm q\omega_a$, in which q = 1, 2, 3, …. The electromagnetic fields at sum (i.e. $\omega_0+q\omega_a$) and difference frequencies (i.e. $\omega_0-q\omega_a$) are known as anti-Stokes and Stokes modes, respectively. In the present analysis, only the first-order Stokes mode (q = 1) is considered; the electron density fluctuations at off-resonant frequencies (with $q\geq 2$) are neglected [24]. Under rotating-wave approximation (RWA),from Eq. (7), the coupled equations are as:

$$\frac{\partial^2 n_{1f}}{\partial t^2}+\nu\frac{\partial n_{1f}}{\partial t}+\bar{\omega}_{pc}^2 n_{1f}$$

$$+\frac{n_0 e k_s^2 u^*}{m\varepsilon_1}(\beta\gamma\delta_1\delta_2 A+\gamma^2E_0^2)E_0E_s^*=-in_{1s}^*k_s\bar{E} \tag{8a}$$

and

$$\frac{\partial^2 n_{1s}}{\partial t^2}+\nu\frac{\partial n_{1s}}{\partial t}+\bar{\omega}_{pc}^2 n_{1s}=in_{1f}^*k_s\bar{E}. \tag{8b}$$

Eqs. (8a) and (8b) clearly illustrate that the slow and fast components (n_{1s}, n_{1f}) of the electron density perturbations are coupled to each other via the pump field ($\bar{E}$). Thus, it is clear that for SBS to occur, the presence of the pump field is the fundamental necessity.

Solving the coupled wave equations (8a) and (8b) and using Eq. (1b), an expression for $n_{1s}$is obtained as:

$$n_{1s}=\frac{n_0k_ak_s(\beta\gamma\delta_1\delta_2A+\gamma^2E_0^2)E_0E_s^*}{2\rho\varepsilon\delta_3(\omega_a^2-k_a^2v_a^2+2i\Gamma_a\omega_a)(\omega_0^2-\omega_c^2+2i\nu\omega_0)}, \tag{9}$$

where $\Omega_{ps}^2=\bar{\omega}_{pc}^2-\omega_s^2$, and $\Omega_{pa}^2=\bar{\omega}_{pc}^2-\omega_a^2$ and

$$\delta_3=1-\frac{(\Omega_{ps}^2-i\nu\omega_s)(\Omega_{pa}^2+i\nu\omega_a)}{k_s^2\bar{E}^2}.$$

From Eq. (2), the components of oscillatory electron fluid velocity in the presence of pump and applied magnetic fields are obtained as:

$$v_{0x}=\frac{\bar{E}}{\nu-i\omega_0}, \tag{10a}$$

and

$$v_{0y}=\frac{(e/m)[\omega_c+(\nu-i\omega_0)]E_0}{[\omega_c^2+(\nu-i\omega_0)^2]}. \tag{10b}$$

The resonant Stokes component of the electron current density due to finite nonlinear polarization of Brillouin medium is deduced (by neglecting the transition dipole moment) as:

$$J_{cd}(\omega_s)=n_{1s}^*ev_{0x}$$

$$=\frac{k_ak_s\omega_p^2(\nu-i\omega_0)(\beta\gamma\delta_1\delta_2A+\gamma^2E_0^2)|E_0|^2E_s^*}{2\rho\delta_3(\omega_a^2-k_a^2v_a^2+2i\Gamma_a\omega_a)(\omega_0^2-\omega_c^2+2i\nu\omega_0)}. \tag{11}$$

2.2. Effective Brillouin susceptibility

The time integral of induced current density yields the nonlinear induced polarization as:

$$P_{cd}(\omega_s) = \int J_{cd}(\omega_s)\, dt = \frac{-J_{cd}(\omega_s)}{i\omega_s}$$

$$= \frac{k_a k_s \omega_p^2 \omega_0^3 (\beta\gamma\delta_1\delta_2 A + \gamma^2 E_0^2)|E_0|^2 E_s^*}{2\rho\omega_s\delta_3(\omega_a^2 - k_a^2 v_a^2 + 2i\Gamma_a\omega_a)(\omega_0^2 - \omega_c^2 + 2i\nu\omega_0)}. \quad (12)$$

Defining the nonlinear induced polarization (at ω_s) as:

$$P_{cd}(\omega_s) = \varepsilon_0 (\chi_B^{(3)})_{cd} |\bar{E}_0|^2 E_s^*,$$

The Brillouin susceptibility $(\chi_B^{(3)})_{cd}$ is given by:

$$(\chi_B^{(3)})_{cd} = \frac{k_a k_s \omega_p^2 \omega_0^3 [\beta\gamma\delta_1\delta_2 A + (2\gamma^2/\eta c\varepsilon_0) I_0]}{2\rho\varepsilon_0\omega_s\delta_3(\omega_a^2 - k_a^2 v_a^2 + 2i\Gamma_a\omega_a)(\omega_0^2 - \omega_c^2 + 2i\nu\omega_0)} \quad (13)$$

where $I_0 = \frac{1}{2}\eta c\varepsilon_0 |E_0|^2$ is the pump intensity.

In addition to $P_{cd}(\omega_s)$, the Brillouin medium also possesses an electrostrictive polarization $P_{es}(\omega_s)$, the origin of which lies in the interaction of the pump wave with the acoustical vibrations generated within the medium. Using Eqs. (1) and (5), we obtain

$$P_{es}(\omega_s) = \frac{k_a k_s \omega_0^4 \gamma^2}{2\rho(\omega_a^2 - k_a^2 v_a^2 + 2i\Gamma_a\omega_a)(\omega_0^2 - \omega_c^2 + 2i\nu\omega_0)} |E_0|^2 E_s^* \quad (14)$$

Consequently, the corresponding Brillouin susceptibility $(\chi_B^{(3)})_{es}$ is given by

$$(\chi_B^{(3)})_{es} = \frac{k_a k_s \omega_0^4 \gamma^2}{2\rho\varepsilon_0(\omega_a^2 - k_a^2 v_a^2 + 2i\Gamma_a\omega_a)(\omega_0^2 - \omega_c^2 + 2i\nu\omega_0)}. \quad (15)$$

The effective Brillouin susceptibility in a Brillouin medium is given by

$$(\chi_B^{(3)})_e = (\chi_B^{(3)})_{es} + (\chi_B^{(3)})_{cd}$$

$$= \frac{k_a k_s \omega_0^4 \gamma^2}{2\rho\varepsilon_0(\omega_a^2 - k_a^2 v_a^2 + 2i\Gamma_a\omega_a)(\omega_0^2 - \omega_c^2 + 2i\nu\omega_0)}\left(1 + \frac{\delta_4\delta_5}{\delta_3}\right) \quad (16)$$

where $\delta_4 = 1 + (\beta/\gamma)\delta_1\delta_2 A$ and $\delta_5 = \frac{2I_0\omega_p^2}{\eta c\varepsilon_0\omega_0\omega_s}$.

One may observe that $(\chi_R^{(3)})_e$ is a complex quantity and it can be expressed as:

$$(\chi_B^{(3)})_e = [(\chi_B^{(3)})_e]_r + i[(\chi_B^{(3)})_e]_i,$$

where $[(\chi_B^{(3)})_e]_r$ and $[(\chi_B^{(3)})_e]_i$ stand for the real and imaginary parts of $(\chi_B^{(3)})_e$, respectively. Rationalizing Eq. (16), we obtain

$$[(\chi_B^{(3)})_e]_r = \frac{k_a k_s \omega_0^4 \gamma^2 (\omega_a^2 - k_a^2 v_a^2)(\omega_0^2 - \omega_c^2)}{2\rho\varepsilon_0[(\omega_a^2 - k_a^2 v_a^2)^2 + 4\Gamma_a^2\omega_a^2][(\omega_0^2 - \omega_c^2)^2 + 4\nu^2\omega_0^2]} \times\left(1 + \frac{\delta_4\delta_5}{\delta_3}\right) \quad (17a)$$

$$[(\chi_B^{(3)})_e]_i = \frac{-2k_a k_s \nu\omega_0^5\omega_a\Gamma_a\gamma^2}{\rho\varepsilon_0[(\omega_a^2 - k_a^2 v_a^2)^2 + 4\Gamma_a^2\omega_a^2][(\omega_0^2 - \omega_c^2)^2 + 4\nu^2\omega_0^2]} \times\left(1 + \frac{\delta_4\delta_5}{\delta_3}\right). \quad (17b)$$

Eqs. (17a) and (17b) show that both $[(\chi_B^{(3)})_e]_r$ as well as $[(\chi_B^{(3)})_e]_i$ are influenced by the piezoelectric coefficient β (via parameter δ_4), the electrostrictive coefficient γ (via parameter δ_4), doping concentration n_0 (via electron-plasma frequency ω_p and hence the parameter δ_3), applied magnetic field B_0 (via electron-cyclotron frequency ω_c, the parameters δ_1 and δ_2) and pump intensity I_0.

2.3. SS and TR Brillouin gain coefficients

At pump intensities well above the threshold intensity, SS-BGC, i.e. $(g_B)_{ss}$ can be obtained as [27]:

$$(g_B)_{ss} = -\frac{k_s}{4\eta^3\varepsilon_0 c}[(\chi_B^{(3)})_e]_i I_0$$

$$= \frac{k_a k_s^2 \nu\omega_0^5\omega_a\Gamma_a\gamma^2 I_0}{2\rho\varepsilon_0^2\eta^3 c[(\omega_a^2 - k_a^2 v_a^2)^2 + 4\Gamma_a^2\omega_a^2][(\omega_0^2 - \omega_c^2)^2 + 4\nu^2\omega_0^2]} \times\left(1 + \frac{\delta_4\delta_5}{\delta_3}\right). \quad (18)$$

Eq. (18) reveals that $(g_B)_{ss}$ increases linearly with I_0. Practically, however, I_0 cannot be increased arbitrary because it may damage the sample. When a semiconductor-plasma is irradiated by an intense long pulsed laser, a frequent outcome is the heat generation [36]. A pump intensity ~ 10^{11} Wm^{-2} of Q-switched 170 ns pulse frequency doubled 10.6 μm CO_2 laser damages InSb at 300 K [37]. The damage threshold intensity of the semiconductor-plasma can be increased by free carrier nonlinear absorption or by reducing the duration of pump pulse [38]. Due to the threshold nature of SBS, it is observed at high pump intensities and hence the pulsed lasers are generally employed in SBS experiments. For SBS and resulting Brillouin amplification to occur, an intense pump wave with ns or sub-ns pulse duration is desired. These pulse durations are of the order of acoustical phonon mode lifetime

($\tau_p \sim \Gamma_a^{-1}$), and under such condition, instead of $(g_B)_{ss}$ alone, $(g_B)_{ss}\Gamma_a$ is more important gain parameter. This parameter suggests an idea of Stokes pulse compression [39]. It is thus clear from above discussion that SBS must be treated under coherent transient excitation regime. TR-BGC, i.e. $(g_B)_{tr}$ of a semiconductor-plasma may be obtained as[29]:

$$(g_B)_{tr} = [2(g_B)_{ss} L\Gamma_a\tau_p]^{1/2} - \Gamma_a\tau_p \; ; \; \Gamma_a\tau_p < (g_B)_{ss} L \, .$$
$$= \left[\frac{k_a k_s^2 \nu\omega_0^5\omega_a\Gamma_a\gamma^2 L\Gamma_a\tau_p I_0}{\rho\varepsilon_0^2\eta^3 c[(\omega_a^2 - k_a^2\nu_a^2)^2 + 4\Gamma_a^2\omega_a^2][(\omega_0^2-\omega_c^2)^2 + 4\nu^2\omega_0^2]} \times\left(1+\frac{\delta_4\delta_5}{\delta_3}\right)^{1/2}\right]^{1/2} - \Gamma_a\tau_p \, . \quad (19)$$

Here Γ_a is the acoustical phonon lifetime, L is the interaction length, τ_p is the pump pulse duration. For backward SBS ($\phi = 180^o$) at very short pump pulse duration ($\tau_p \le 10^{-10}$ s), the interaction length can be replaced by $c\tau_p/2$, where c is the speed of light in the crystal lattice and is given by $c_0/(\varepsilon_1)^{1/2}$.

2.4. Threshold pump intensity and optimum pulse duration for TR Brillouin gain

The threshold pump intensity for onset of the backward SBS is obtained, by making $(g_B)_{tr} = 0$ in Eq. (19), as:

$$I_{0,th,tr} = \frac{\Gamma_a\tau_p}{2c(g_B)_{ss}} I_0$$
$$= \frac{\Gamma_a\tau_p}{2c}\left[\frac{k_a k_s^2 \nu\omega_0^5\omega_a\Gamma_a\gamma^2}{2\rho\varepsilon_0^2\eta^3 c[(\omega_a^2 - k_a^2\nu_a^2)^2 + 4\Gamma_a^2\omega_a^2][(\omega_0^2-\omega_c^2)^2 + 4\nu^2\omega_0^2]} \times\left(1+\frac{\delta_4\delta_5}{\delta_3}\right)\right]^{-1} . \quad (20)$$

Using $\Gamma_a = 2\times10^{10}$ s^{-1} and $(g_B)_{ss} = 1.6\times10^2$ m^{-1} at $I_0 = 3.7\times10^{10}$ Wm^{-2} for n-InSb-CO_2 laser system and Eq. (20), we obtain the threshold intensity for the onset of TR-SBS as 4.7×10^{11} Wm^{-2}.

However, for $\tau_p \ge 10^{-9}$ s, the cell length can be taken equal to L, and under such a condition we obtain

$$(g_B)_{tr} = (\Gamma_a\tau_p)^{1/2}[(2(g_B)_{ss}L)^{1/2} - (\Gamma_a\tau_p)^{1/2}]$$
$$= \left[\frac{2k_a k_s^2 \nu\omega_0^5\omega_a\Gamma_a^2\tau_p\gamma^2 L I_0}{\rho\varepsilon_0^2\eta^3 c[(\omega_a^2 - k_a^2\nu_a^2)^2 + 4\Gamma_a^2\omega_a^2][(\omega_0^2-\omega_c^2)^2 + 4\nu^2\omega_0^2]} \times\left(1+\frac{\delta_4\delta_5}{\delta_3}\right)\right]^{1/2} - \Gamma_a\tau_p \, . \quad (21)$$

The above expression gives an idea about the optimum pulse duration $(\tau_p)_{opt}$ above which no Brillouin gain could be achieved by making $(g_B)_{tr} = 0$ in Eq. (21), as:

$$(\tau_p)_{opt} \approx \frac{(g_B)_{ss}}{\Gamma_a}$$
$$\approx \frac{k_a k_s^2 \nu\omega_0^5\omega_a\gamma^2 I_0}{2\rho\varepsilon_0^2\eta^3 c[(\omega_a^2 - k_a^2\nu_a^2)^2 + 4\Gamma_a^2\omega_a^2][(\omega_0^2-\omega_c^2)^2 + 4\nu^2\omega_0^2]} \times\left(1+\frac{\delta_4\delta_5}{\delta_3}\right) . \quad (22)$$

A calculation for n-InSb-CO_2 laser system using the values given earlier and L = 1 mm yields $(\tau_p)_{opt} = 3.9\times10^{-19} I_0$ s. This value of $(\tau_p)_{opt}$ not only explains the fact that Brillouin gain vanishes at longer pulse duration but also suggests that optimum pulse duration can be increased by increasing the intensity of the pump wave.

3. Results and discussion

The theoretical formulations as developed in the previous section will be analyzed in this section to study SBS in piezoelectric semiconductor magneto-plasmas.

The SBS parameters ($(g_B)_{ss}$, $(g_B)_{tr}$, $I_{0,th,tr}$, and $(\tau_p)_{opt}$) in the presence of magnetic field ($B_0 \ne 0$) and finiteness of piezoelectric coefficient ($\beta \ne 0$) can be studied from Eqs. (18) – (22). However, in the absence of either/both magnetic field and piezoelectricity, the SBS parameters can be obtained by following substitutions:

(i) In the absence of magnetic field ($B_0 = 0$): $\omega_c = 0$, $\delta_1 = 0$, $\delta_2 = 0$, hence $\delta_3 = 0$ and $\delta_4 = 0$.

(ii) In the absence of piezoelectricity ($\beta = 0$): $\delta_4 = 0$.

With these substitutions, it comes out that the SBS parameters for cases:

(a) absence of magnetic field ($B_0 = 0$) and presence of piezoelectricity ($\beta \ne 0$), and

(b) absence of both magnetic field ($B_0 = 0$) and piezoelectricity ($\beta = 0$) are identical.

Thus it may be concluded that the piezoelectric contributions to SBS are only in the presence of magnetic field. Moreover, the finiteness of electrostrictive coefficient ($\gamma \ne 0$) is the foremost condition for SBS to occur. The SBS parameters become independent of doping concentration n_0 (via ω_p) for the cases when either/both $B_0 = 0$ or $\beta = 0$ (i.e. absence of either/both magnetic field and piezoelectricity).

For numerical analysis, we consider the irradiation of *n*-InSb sample by 10.6 μm CO_2 at 77 K. The other material parameters of n-InSb crystal are taken as follows [23]:

$$m = 0.014m_0,\ \rho = 5.8\times10^3\ \text{kg m}^{-3},$$
$$\varepsilon_1 = 15.8,\ v_a = 4\times10^3\ \text{ms}^{-1},$$
$$\beta = 0.054\ \text{Cm}^{-2},\ \gamma = 5\times10^{10}\ \text{s}^{-1},$$
$$\Gamma_a = 2\times10^{10}\ \text{s}^{-1},\ \nu = 4\times10^{11}\ \text{s}^{-1},$$
$$\omega_a = 2\times10^{11}\ \text{s}^{-1},\ \omega_0 = 1.78\times10^{14}\ \text{s}^{-1}.$$

Eqs. (18) – (22) contain some common parameters which significantly influence the SBS parameters. These terms can be explained as follows:

(i) In term $1+(\delta_4\delta_5/\delta_3)$, the parameter δ_5 is intensity dependent. It is interesting to note that for material parameters of n-InSb-CO_2 laser system given above, at pump intensities $I_0 < I_c (= 5.15\times10^{13}\ \text{Wm}^{-2})$, $(\delta_4\delta_5/\delta_3) < 1$; the parameter $\delta_4\delta_5/\delta_3$ can be neglected in comparison to unity and the SBS parameters become dependent on γ only. However, at pump intensities $I_0 > I_c$, $(\delta_4\delta_5/\delta_3) > 1$; the parameter $\delta_4\delta_5/\delta_3$ plays important role in the analysis and the SBS parameters depends on β as well as γ (via parameter δ_4).

(ii) The term $(\omega_a^2 - k_a^2 v_a^2)^2$ occurs due to dispersion characteristics of the acoustical phonon mode. For material parameters of n-InSb-CO_2 laser system given above and for $k_a = 5\times10^7\ \text{m}^{-1}$, $\omega_a \approx k_a v_a$ and the term $(\omega_a^2 - k_a^2 v_a^2)^2 \to 0$ yielding high SS- and TR-BGCs at lower pump intensities.

(iii) The parameter $(\omega_0^2 - \omega_c^2)^2$ becomes important when magnetic field dependent electron-cyclotron frequency becomes comparable to pump wave frequency. For material parameters of n-InSb-CO_2 laser system given above and at $B_0 = 14.2\,\text{T}$, $\omega_c^2 \approx \omega_0^2$ and the term $(\omega_0^2 - \omega_c^2)^2 \to 0$ yielding high SS- and TR-BGCs at lower pump intensities.

(iv) The parameter Ω_{ps}^2 (in term δ_3), for material parameters of n-InSb-CO_2 laser system given above, by increasing B_0 continuously in the considered range and decreasing n_0 proportionally, allows to resonate coupled plasmon-cyclotron mode frequency at Stokes mode frequency, i.e. $\bar{\omega}_{pc}^2 \sim \omega_s^2$.

(v) The parameter Ω_{pa}^2 (in term δ_3), allows to resonate coupled plasmon-cyclotron mode frequency at acoustical mode frequency, i.e. $\bar{\omega}_{pc}^2 \sim \omega_a^2$; but for the considered range of B_0, extremely high values of n_0 are required. The high values of doping concentration will lead to diffusion effects and the theoretical formulation developed here, thereby needed a modification.

At $\omega_c \sim \omega_0$, we obtain the following ratios:

$$\frac{(I_{0,th,tr})_{\omega_a = k_a v_a}}{(I_{0,th,tr})_{\omega_a \neq k_a v_a}} = 1.98\times10^{-2},$$
$$\frac{[(g_B)_{ss}]_{\omega_a = k_a v_a}}{[(g_B)_{ss}]_{\omega_a \neq k_a v_a}} = 2.55\times10^{2}, \text{ and}$$
$$\frac{[(g_B)_{tr}]_{\omega_a = k_a v_a}}{[(g_{tr})_{ss}]_{\omega_a \neq k_a v_a}} = 2.49\times10^{2}.$$

At $\omega_a = k_a v_a$, the following ratios are obtained:

$$(I_{0,th,tr})_{\substack{\omega_c=\omega_c,\\ \beta\neq0}} : (I_{0,th,tr})_{\substack{\omega_c=\omega_c,\\ \beta=0}} : (I_{0,th,tr})_{\substack{\omega_c=0,\\ \beta=0\text{or}\beta\neq0}} = 9.7\times10^{-2} : 2.7\times10^{-2} : 1$$
$$[(g_B)_{ss}]_{\substack{\omega_c=\omega_c,\\ \beta\neq0}} : [(g_B)_{ss}]_{\substack{\omega_c=\omega_c,\\ \beta=0}} : [(g_B)_{ss}]_{\substack{\omega_c=0,\\ \beta=0\text{or}\beta\neq0}} = 1.2\times10^{3} : 4.6\times10^{2} : 1$$
$$[(g_B)_{tr}]_{\substack{\omega_c=\omega_c,\\ \beta\neq0}} : [(g_{tr})_{ss}]_{\substack{\omega_c=\omega_c,\\ \beta=0}} : [(g_{tr})_{ss}]_{\substack{\omega_c=0,\\ \beta=0\text{or}\beta\neq0}} = 1.1\times10^{3} : 4.4\times10^{2} : 1$$

Using Eqs. (18) – (22), the dependence of SS- and TR-BGCs on controllable parameters such as doping concentration (n_0), applied magnetic field (B_0), magnetic field inclination (θ), scattering angle (ϕ), and pump pulse duration (τ_p) is explored in detail. The range of magnetic field considered is 0T ≤ B_0≤ 18T.The magnetic field in this range may be easily produced in the laboratory. It should be worth pointing out that Generazio and Spector [40] studied the phenomenon of free carrier absorption for n-InSb-CO_2 and n-InSb-CO laser systems at 77 K by placing the sample in an external magnetic field B_0≤ 20 T; without any optical damage of the crystal and/or change in propagation characteristics of the laser beam.

The results are plotted in Figs. 2 – 7.

Fig. 2 shows the variation of $(g_B)_{ss}$ and $(g_B)_{tr}$ with magnetic field (B_0) for two different doping concentrations. It can be observed that both $(g_B)_{ss}$ and $(g_B)_{tr}$ show similar nature of curves throughout the plotted regime of B_0. The nature of the curves can be explained as follows: By keeping n_0 fixed and varying B_0, we observed that SS- and TR-BGCs are comparatively smaller and remain independent of magnetic field in the regimes $0 < B_0 < 9.5\text{T}$ and $0 < B_0 < 2.7\text{T}$ for $n_0 = 2\times10^{19}\ \text{m}^{-3}$ and $3\times10^{19}\ \text{m}^{-3}$, respectively. With further increasing B_0 beyond this value, SS- and TR-BGCs start increasing, achieving their peaks at B_0 = 10.5T and 3.7T for $n_0 = 2\times10^{19}\ \text{m}^{-3}$ and $3\times10^{19}\ \text{m}^{-3}$, respectively. With further slightly increasing B_0 beyond these values, SS- and TR-BGCs decrease sharply and attain their previously lower value at B_0 = 11.5T and 4.7T for

$n_0 = 2\times10^{19}$ m^{-3} and 3×10^{19} m^{-3}, respectively and remain constant for B_0 = 13T.

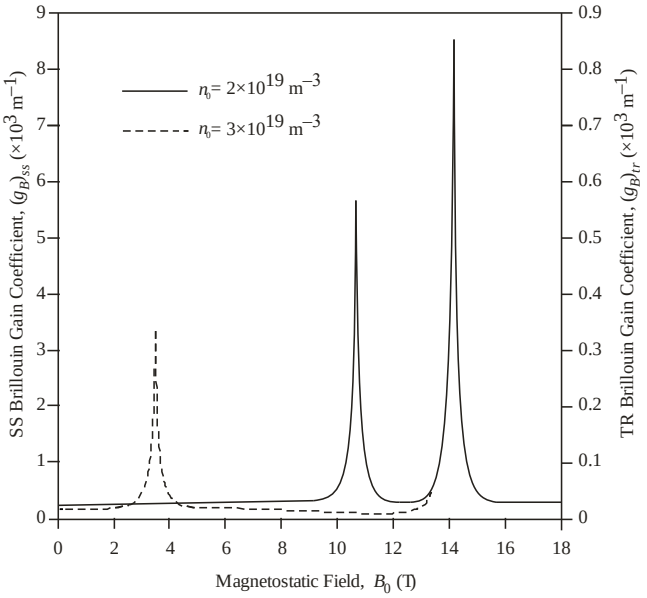

Fig. 2. Variation of $(g_B)_{ss}$ *and* $(g_B)_{tr}$ *with* B_0 *for* $n_0 = 2\times10^{19}$ *m*$^{-3}$ *and* 3×10^{19} *m*$^{-3}$ *in n-InSb crystal. Here* $k_a = 5\times10^7$ *m*$^{-1}$, $\theta = 60^o$, $\phi = 45^o$, $\tau_p = 2\times10^{-10}$ *s, and* $I_0 = 7\times10^{12}$ *Wm*$^{-2}$

This distinct behaviour of BGCs occur due to resonance condition: $\bar{\omega}_{pc}^2 \sim \omega_s^2$. An exciting aspect of this resonance condition is the interaction between electron-plasmon oscillator and electron-cyclotron oscillator. We considered this as hybrid oscillator. When the pump field interacts with hybrid oscillator, as a consequence, ω_p and ω_c dependent Stokes signal (at ω_s) is generated. It is beneficial to move ω_s to an obtainable spectral regime in proportion to: (i) n_0 (or ω_p) for fixed B_0 (or ω_c), (ii) B_0 (or ω_c) for fixed n_0 (or ω_p), and (iii) combination of n_0 and B_0 both. By continuously increasing n_0 (via ω_p and hence $\bar{\omega}_{pc}^2$) and decreasing B_0 (via ω_c and hence $\bar{\omega}_{pc}^2$) in the same proportion maintains the resonance condition at a fixed value of ω_s. Further, by continuously increasing n_0 and decreasing B_0 without maintaining their proportion shifts the value of ω_s. In the present case, by continuously increasing ω_s form 2×10^{19} m^{-3} to 3×10^{19} m^{-3} and decreasing B_0 from 10.5T to 3.7T maintains the resonance condition $\bar{\omega}_{pc}^2 \sim \omega_s^2$ at a fixed value of ω_s. Ultimately, at $n_0 = 3.3\times10^{19}$ m^{-3}, the resonance occurs around B_0 = 0T for a fixed value of ω_s. For $n_0 > 3.3\times10^{19}$ m^{-3}, the resonance condition shifts the value of ω_s.

At B_0 = 13.5T, SS- and TR-BGCs corresponding to two different values of doping concentration as reported above become equal and exhibit common behaviour independent of doping concentration for $B_0 \geq 13.5$T. SS- and TR-BGCs exhibit a common peak at B_0 = 14.2T. This peak occurs due to resonance condition: $\omega_c^2 \sim \omega_0^2$. In the proximity of resonance, the electron's drift velocity (which is the function of B_0) increases, attains a value higher than acoustical phonon mode velocity and due to this the rate of energy flow from pump to acoustical phonon mode increases, and consequently the amplification of acoustical phonon mode occurs. Eventually, the interaction between pump field and amplified acoustical phonon mode takes place and the amplitude of scattered Stokes mode enhances adequately thereby enhancing SS- and TR-BGCs.

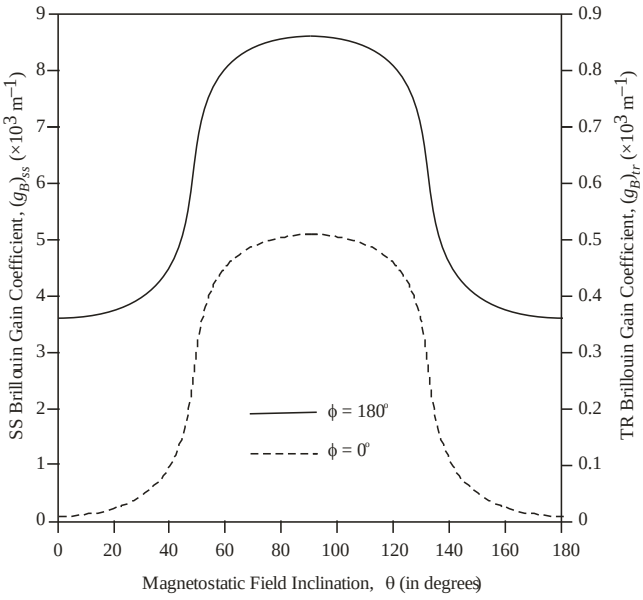

Fig. 3: Variation of $(g_B)_{ss}$ *and* $(g_B)_{tr}$ *with* θ *for* $\phi = 0^o$ *and* 180^o *in n-InSb crystal. Here* $k_a = 5\times10^7$ *m*$^{-1}$, $n_0 = 2\times10^{19}$ *m*$^{-3}$, $\phi = 45^o$, $\tau_p = 2\times10^{-10}$ *s and* $I_0 = 7\times10^{12}$ *Wm*$^{-2}$

The most significant feature of the result is enhancement of SS- and TR-BGCs around resonances by varying simultaneously/independently doping concentration and magnetic field in semiconductors-plasmas. The results obtained in Fig. 2 permits the tuning of scattered Stokes mode over a broad range of frequencies and reveal the opportunity of fabrication of frequency converters based on Brillouin amplification as well as tunable Brillouin oscillators.

Fig. 3 shows the variation of $(g_B)_{ss}$ and $(g_B)_{tr}$ with magnetic field inclination (Θ) for $\phi = 0^o$ (forward scattering) and $\phi = 180^o$ (backward scattering). It can be

observed that in both the cases, SS- and TR-BGCs are comparatively smaller in case of Faraday geometry (i.e. $\theta = 0^o$). SS- and TR-BGCs continuously increase with θ in the regime $\theta < 90^o$, achieving maximum at $\theta = 90^o$ and decrease with θ in the regime $\theta > 90^o$. The rate of rise (fall) of SS- and TR-BGCs is higher in the regimes $20^o < \theta < 70^o$ ($110^o < \theta < 160^o$). The curves are symmetrical about $\theta = 90^o$. The curves infer that the contribution of magnetic Lorentz force, which plays a significant role in modifying the electron's drift velocity, consequently energy transfer from pump to scattered Stokes wave and subsequently enhancing SS- and TR-BGCs is maximum in case of Voigt geometry (i.e. $\theta = 90^o$). Moreover, SS- and TR-BGCs are higher under Voigt geometry than under Faraday geometry.

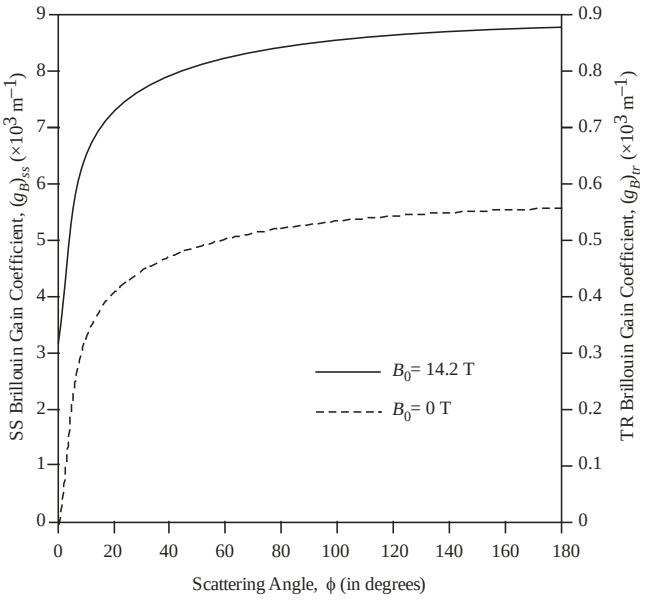

Fig. 4. Variation of $(g_B)_{ss}$ and $(g_B)_{tr}$ with ϕ for $B_0 = 0$ T and 14.2T. Here $k_a = 5\times10^7$ m^{-1}, $n_0 = 2\times10^{19}$ m^{-3}, $\theta = 60^o$, $\tau_p = 2\times10^{-10}$ s and $I_0 = 7\times10^{12}$ Wm^{-2}

Fig. 4 shows the variation of $(g_B)_{ss}$ and $(g_B)_{tr}$ with scattering angle (ϕ) in the absence (B_0 = 0T) and presence (B_0 = 14.2T) of magnetic field. It can be observed that in both the cases, SS- and TR-BGCs are larger in the forward scattering direction (i.e., $\phi = 0^o$). However, Stokes mode grows exponentially between $0^o < \phi < 40^o$ and thereafter the growth rate slows down, finally saturate around $\phi = 180^o$. SS- and TR-BGCs in case of backward scattering are higher than in case of forward scattering. In addition, SS- and TR-BGCs are four times higher in the presence of magnetic field than in its absence throughout the plotted range of scattering angle.

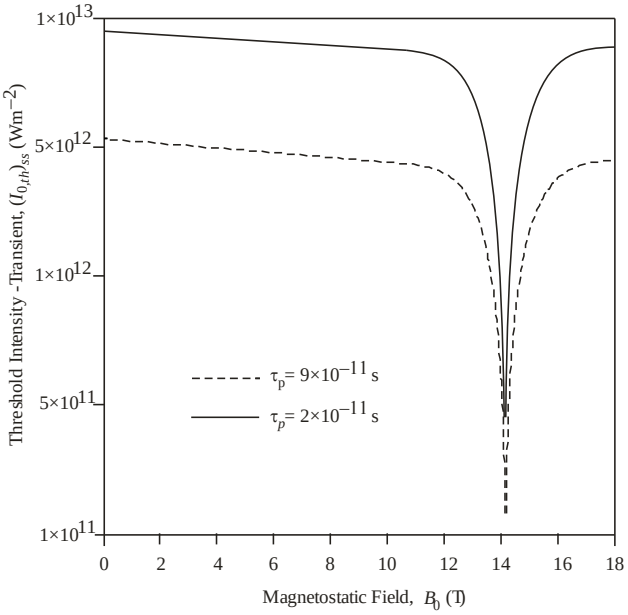

Fig. 5. Variation of $(I_{0,th})_{tr}$ with B_0 for $\tau_p = 2\times10^{-10}$ s and 9×10^{-11} s. Here $k_a = 5\times10^7$ m^{-1}, $n_0 = 5\times10^{19}$ m^{-3}, $\theta = 60^o$, $\phi = 45^o$.

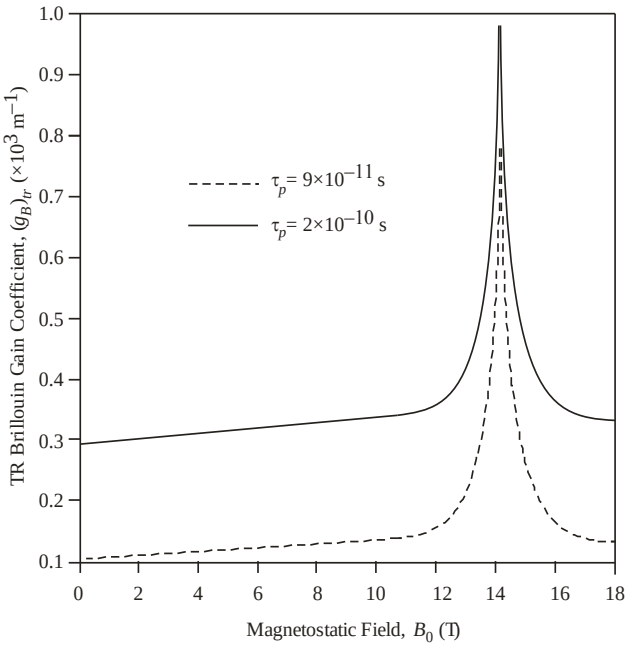

Fig. 6. Variation of $(g_B)_{tr}$ with B_0 for $\tau_p = 2\times10^{-10}$ s and 9×10^{-11} s. Here $k_a = 5\times10^7$ m^{-1}, $n_0 = 5\times10^{19}$ m^{-3}, $\theta = 60^o$, $\phi = 45^o$, and $I_0 = 7\times10^{12}$ Wm^{-2}

Fig. 5 shows the variation of threshold intensity $(I_{0,th})_{tr}$) for the onset of TR-SBS with magnetic field (B_0) for two different pump pulse durations. It can be observed

that in both the cases, $(I_{0,th})_{tr}$ decreases gradually with B_0 for B_0 < 11T. This feature indicates that the Lorentz contribution is quite small when $\omega_c < \omega_0$. However, when ω_c approaches ω_0, the Lorentz contribution is very effective to minimize the value of $(I_{0,th})_{tr}$. When $\omega_c > \omega_0$ (i.e. B_0> 14.2T), $\omega_c > \omega_0$ increases sharply due to departure from the resonance and subsequently it remains constant even at comparatively large magnetic field. A comparison between the two curves reveals that $\omega_c > \omega_0$ decreases with decreasing pump pulse duration.

Fig. 6 shows the variation of $(g_B)_{tr}$ with magnetic field (B_0) for two different pump pulse durations. It can be observed that in both the cases, $(g_B)_{tr}$ increases gradually with B_0 for B_0< 11T. This feature indicates that the Lorentz contribution is quite small when $\omega_c < \omega_0$. However, when ω_c approaches ω_0, the Lorentz contribution is very effective to enhance the value of $(g_B)_{tr}$. When $\omega_c > \omega_0$ (i.e. B_0> 14.2T), $(g_B)_{tr}$ decreases sharply due to departure from the resonance and subsequently it remains constant even at comparatively large magnetic field. A comparison between the two curves reveals that $(g_B)_{tr}$ increases with increasing pump pulse duration.

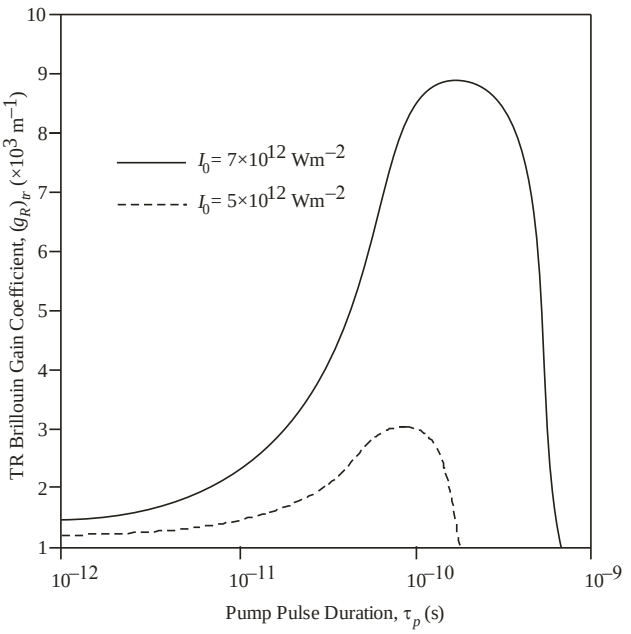

Fig. 7. Variation of $(g_B)_{tr}$ with τ_p at $I_0 = 5\times10^{12}$ Wm^{-2} and 7×10^{12} Wm^{-2}. Here $k_a = 5\times10^7$ m^{-1}, $n_0 = 5\times10^{19}$ m^{-3}, $B_0 = 14.2$ T, $\theta = 60^\circ$, and $\phi = 45^\circ$

Fig. 7 shows the variation of $(g_B)_{tr}$ with pump pulse duration (in the range $10^{-12}\text{s} \le \tau_p \le 10^{-9}\text{s}$) for two different pump intensities. We observed that for fixed I_0, $(g_B)_{tr}$ increases with τ_p and at a certain value of τ_p, $(g_B)_{tr}$ attains a certain maximum value which remains constant over a certain range of τ_p. Such regimes may be regarded as quasi-SS or quasi-saturation regimes. The rise in I_0 shifts the gain saturation regime towards higher values of τ_p. Keeping I_0 fixed, if τ_p is chosen beyond the quasi-saturation regime, $(g_B)_{tr}$ diminishes very rapidly.

4. Conclusions

The current paper is an analytical investigation of SS- and TR-BGCs in weakly-piezoelectric semiconductor magneto-plasmas. Following important conclusions may be drawn from the study:

1. The analysis offers two achievable resonance conditions ($\bar{\omega}_{pc}^2 \sim \omega_s^2, \omega_c^2 \sim \omega_0^2$) at which significant enhancement of SS- and TR-BGCs can be obtained.
2. The threshold pump intensity for exciting TR-SBS is three orders of magnitude is smaller in presence of both piezoelectricity and magnetic field (around resonance), two orders of magnitude smaller in presence of magnetic field and absence of piezoelectricity than the absence of magnetic field and presence/absence of piezoelectricity.
3. SS- and TR-BGCs are three orders of magnitude larger in presence of both piezoelectricity and magnetic field (around resonance), two orders of magnitude larger in presence of magnetic field and absence of piezoelectricity than the absence of magnetic field and presence/absence of piezoelectricity.
4. SS- and TR-BGCs are one order of magnitude higher under Voigt geometry than under Faraday geometry, one order of magnitude higher for backward scattering than forward scattering.
5. The rise in pump intensity shifts the gain saturation regime towards higher values of pump pulse duration. For example, in n-InSb semiconductor-plasma, the quasi-saturation regime which occurs around $\tau_p = 9\times10^{-11}$ s at $I_0 = 5\times10^{12}$ Wm^{-2} shifts to $\tau_p = 2\times10^{-10}$ s at $I_0 = 7\times10^{12}$ Wm^{-2}.
6. The technological potentiality of weakly-piezoelectric semiconductor magneto-plasmas as hosts for fabrication of efficient nonlinear devices such as frequency converters, Brillouin amplifiers and oscillators etc. based on Brillouin nonlinearities is established.

Acknowledgements

One of the authors (M. Singh) is thankful to Director General, Department of Higher Education, Haryana for kind cooperation to carry out this research work.

References

[1] J. Ji, H. Wang, J. Cui, M. Yu, Z. Yang, L. Bai, Photon. Netw. Commun. **38**, 14 (2019).

[2] M. Ono, M. Hata, M. Tsunekawa, K. Nozaki, H. Sumikura, H. Chiba, M. Notomi, Nature Photonics **14**, 37 (2020).

[3] T. Hao, Y. Liu, J. Tang, Q. Cen, W. Li, N. Zhu, Y. Dai, J. Capmany, Y. Yao, M. Li, Adv. Photonics **2**, 044001 (2020).

[4] D. Tan, K.N. Sharafudeen, Y. Yue, J. Qiu, Prog. Material Science **76**, 154 (2016).

[5] R.Y. Chiao, C.H. Townes, B.P. Stoicheff, Phys. Rev. Lett. **21**, 592 (1964).

[6] Q. Guo, Z. Lu, Y. Wang, Appl. Phys. Lett. **96**, 221107 (2010).

[7] T. Omatsu, H.J. Kong, S. Park, S. Cha, H. Yoshida, K. Tsubakimoto, H. Fujita, M. Miyanaga, M. Nakatsuka, Y. Wang, Z. Li, Z. Zheng, Y. Zhang, M. Kalal, O. Slezak, M. Ahihara, T. Yoshino, K. Hayashi, Y. Tokozane, M. Okida, K. Miyamoto, K. Toyoda, A. A. Grabar, Md. M. Kabir, Y. Oishi, H. Suzuki, F. Kannari, C. Schaefer, K. R. Pandiri, M. Katsuragawa, Y. L. Wang, Z. W. Lu, S. Y. Wang, Z. X. Zheng, W. M. He, D. Y. Lin, W. L. J. Hasi, X. Y. Guo, H. H. Lu, M. L. Fu, S. Gong, X. Z. Geng, R. P. Sharma, P. Sharma, S. Rajput, A. K. Bhardwaj, C. Y. Zhu, W. Gao, Laser Part. Beams **30**(1), 117 (2012).

[8] A. M. Scott, K. D. Ridley, IEEE J. Quantum Electron. **25**, 438 (1989).

[9] S. Bhan, S.P. Singh, V. Kumar, M. Singh, Optik**184**, 464 019).

[10] A. Brignon, H. Jean-Pierre, Phase Conjugate Laser Optics, John Wiley & Sons, New York, 2004.

[11] K. Shimizu, T. Horiguchi, Y. Koyamada, T. Kurashima, Opt. Lett. **18**, 185 (1993).

[12] X. Bao, L. Chen, Sensors **12**, 8601 (2012).

[13] M. Singh, J.Gahlawat, A. Sangwan, N. Singh, M. Singh, Nonlinear optical susceptibilities of a piezoelectric semiconductor magneto-plasma, in Recent Trends in Materials and Devices. ed. by V. K. Jain, S. Rattan, A. Verma (Springer Proceedings in Physics, Springer, Singapore, 2020) vol. 256.

[14] M. R. Edwards, Q. Jia, J. M. Mikhailova, N. J. Fisch, Phys. Plasmas **23**, 083122 (2016).

[15] G. Marcus, S. Pearl, G. Pasmanik, J. Appl. Phys. **103**, 103105 (2008).

[16] M. H. Al-Mansoori, A. Al-Sheriyani, S. Al-Nassri, F. N. Hasoon, Laser Phys. **27**, 065112 (2017).

[17] B. C. Rodgers, T. H. Russell, W. B. Roh, Opt. Lett. **24**, 1124 (1999).

[18] S. Park, S. Cha, J. Oh, H. Lee, H. Anh, K. S. Churn, H. J. Kong, Opt. Express **24**, 8641 (2016).

[19] M. Gonzalez-Herraez, K. Y. Song, L. Thevenaz, Appl. Phys. Lett. **87**, 081113 (2005).

[20] W. Loh, S. Yegnanarayanan, F. O'Donnell, P. W. Juodawlkis, Optica **6**, 152 (2019).

[21] H. Ahmad, S. N. Aidit, Z. C. Tiu, Opt. Laser Tech. **99**, 52 (2018).

[22] I. Remer, L. Cohen, A. Bilenca, J. Vis. Exp. **127**, 55527 (2017).

[23] M. Salimullah, T. Ferdousi, F. Majid, Phys. Rev. B **50**, 14104 (1994).

[24] M. Singh, P. Aghamkar, N. Kishore, P. K. Sen, Opt. Laser Tech. **40**, 215 (2008).

[25] C. Uzma, I. Zeba, H. A. Shah, M. Salimullah, J. Appl. Phys. **105**, 013307 (2009).

[26] S. Ghosh, G. R. Sharma, P. Khare, M. Salimullah, Physica B: Cond. Matter **351**, 163 (2004).

[27] M. Singh, M. Singh, Iran. J. Sci. Technol. Trans. Sci. **45**, 373 (2021).

[28] Y. Xu, L. Zhou, L. Lu, J. Chen, B. M. A. Rahman, J. Phys. D Appl. Phys. **52**, 184001 (2019).

[29] C. S. Wang, Quantum Electronics. H. Rabin. C. L. Tang (eds.) Academic Press, New York, 1975.

[30] S. G. Chefranov, A. S. Chefranov, Hydrodynamic Methods and Exact Solutions in Applications to the Electromagnetic Field Theory in Medium. In: Nonlinear Optics – Novel Results in Field Theory in Medium, B. Lembrikov (ed.). Intechopen, UK, 2020.

[31] A. Rasheed, M. Jamil, M. Siddique, F. Huda, Y. D. Jung, Phys. Plasmas **21**, 062107 (2014).

[32] M. A. Moghanjoughi, Phys. Plasmas **18**, 012701 (2011).

[33] F. Hass, A. Bret, Europhys. Lett. **97**, 26001 (2012).

[34] S. Ghosh, S. Dubey, R. Vanshpal, Chin. J. Phys. **51**, 1251 (2013).

[35] D. Singh, B. S. Sharma, M. Singh, J. Opt. (2022) https://doi.org/10.1007/s12596-022-00833-z.

[36] J. M. Mayer, F. J. Bartoli, M. R. Kruer, Phys. Rev. B **21**, 1559 (1980).

[37] M. Kruer, L. Esterowitz, F. Bartoli, R. Allea, The Role of Carrier Diffusion in Laser Damage of Semiconductor Materials. In: Laser Induced Damage in Optical Materials, A. J. Glass and A. H. Guenther (eds.), NBS Special Publication No. 509, Washington, 1977.

[38] T. F. Boggess, A. Smirl, S. Moss, I. Boyd, E. V. Stryland, IEEE J. Quantum Electron. **21**, 488 (1985).

[39] D. Phol, W. Kaiser, Phys. Rev. B **1**, 31 (1970).

[40] E. R. Generazio, H. N. Spector, Phys. Rev. **20**, 5162 (1979).

*Corresponding author: msgur_18@yahoo.com